ONLINE SUPPLEMENT December 2019

In infants with severe bronchiolitis: Dual-transcriptomic profiling of nasopharyngeal microbiome and host response

Michimasa Fujiogi; Carlos A. Camargo Jr.; James P. Bernot; Robert J Freishtat; Brennan Harmon; Jonathan M. Mansbach; Eduardo Castro-Nallar; Marcos Perez-Losada; and Kohei Hasegawa, MD, MPH

SUPPLEMENTAL METHODS

Design, Setting, and Sample

We analyzed data from an ongoing multicenter prospective cohort study of infants (aged <12 months) with severe bronchiolitis—the 35th Multicenter Airway Research Collaboration (MARC-35).(1,2) Using a standardized protocol, site investigators at 17 sites across 14 U.S. states enrolled 1,016 infants hospitalized with an attending physician's diagnosis of bronchiolitis during three consecutive bronchiolitis seasons (from November 1 to April 30) in 2011-2014. Bronchiolitis was defined by the American Academy of Pediatrics guidelines: acute respiratory illness with some combination of rhinitis, cough, tachypnea, wheezing, crackles, and retractions. (3) We excluded infants with known heart–lung disease, immunodeficiency, immunosuppression, or gestational age <32 weeks, those who were transferred to a participating hospital 24 hours after the original hospitalization, or those who were consented 24 hours after hospitalization. All patients were treated at the discretion of the treating physicians. The institutional review board at each of the participating hospitals approved the study. Written informed consent was obtained from the parent or guardian.

In the current proof-of-concept study, we performed dual-transcriptomic profiling of the nasopharyngeal samples from five infants with RSV infection and five infants with sole RV infection (i.e., no co-infecting RSV) in MARC-35.

Data Collection

At the index hospitalization, investigators conducted a structured interview that collected patients' demographic characteristics, medical and family history, and details of the acute illness. Emergency department and hospital medical record reviews provided further clinical data, such

as vital signs, physical examination, medical management, and disposition. Review of medical records was performed, after successful completion of training (lecture, practice charts), by board-certified physicians (e.g., from pediatric pulmonary, allergy/ immunology). All data were reviewed at the EMNet Coordinating Center at Massachusetts General Hospital (Boston, MA), and site investigators were queried about missing data and discrepancies identified by manual data checks.

Nasopharyngeal Sampling

On the basis of evidence that upper airway microbiome and inflammatory response are indicative of those in the lower respiratory tract,(4-6) we investigated nasopharyngeal airway specimens. In addition to the clinical data above, investigators also collected nasopharyngeal airway samples within 24 hours of hospitalization by using a standardized protocol that was utilized in a previous cohort study of children with bronchiolitis.(2) All of the sites used the same collection equipment (Medline Industries, Mundelein, IL) and collected the samples within 24 hours of a child's arrival on the medical ward or intensive care unit. These samples underwent real-time polymerase chain reaction (RT-PCR) (for respiratory virus testing) and dual-transcriptomics profiling.

Respiratory Virus Measurement

We identified respiratory viruses by using singleplex or duplex two-step RT-PCR at Baylor College of Medicine (Houston, TX, USA). We used real-time reverse transcriptase-PCR to detect RNA respiratory viruses, including RSV,(7,8) RV,(9) and 12 other RNA viruses. All RT-PCR assays were tested in duplicate and samples with incongruent values (one well positive)

were retested. To reduce carryover contamination, sample preparation, RNA/DNA extraction, cDNA, and amplification were performed in separate areas. All PCR runs had extraction and reagent positive and negative controls.

Dual-transcriptomics Profiling with RNA Sequencing (RNAseq)

We extracted total RNA using Trizol reagent (ThermoFisher Scientific, Waltham, MA). We examined RNA quality by measuring 260/280 absorbance ratio on the NanoDrop 2000 Spectrophotometer (ThermoFisher Scientific) and by running the RNA on the Agilent Bioanalyzer 2100 (Agilent, Palo Alto, CA) using the RNA 6000 Nano kit. Total RNA underwent DNase treatment and rRNA reduction (Illumina Ribo-Zero Gold rRNA Removal Kit [Epidemiology]) before sequencing library preparation using llumina TruSeq Stranded Total RNA Library Prep Kit and sequencing on a HiSeq 4000 sequencer (Illumina, San Diego, CA).

We preprocessed the raw reads using PRINSEQ-lite 0.20.4 (trimming reads and bases <25 PHRED, removing exact duplicates, reads with undetermined bases, and low complexity reads using Dust filter=30).(10) We aligned the filtered reads to the human genome (hg19) using Bowtie2 (--very-sensitive-local).(11) We used the microbial reads for downstream analyses of microbiome composition and function while we utilized the human reads for downstream analyses of host differential gene expression.

Statistical Analysis

Microbiome *compositional profiling*

We used microbial RNA data to infer the microbiome composition with PathoScope.(12-14) In brief, we examined potential contamination in silico when running PathoScope. We

discarded the transcripts that did not align to the human reference genome hg19 for the host gene expression analysis and to unique fungal, prokaryotic, protozoan, or viral genomes available in GenBank for the microbiome compositional and functional profiling analyses. Next, we constructed a "target" genome library containing all unique fungal, prokaryotic, protozoan, and viral genomes available in GenBank. Then, we aligned the clean microbial reads to our target using Bowtie2 (−−very-sensitive-local-k 100 –score- min L,20,1.0).(11) We used the identified taxonomic profiles to characterize the microbiome composition in each patient. We converted the sequence abundances and taxonomy to a BIOM file for subsequent analyses and all singletons were eliminated. We normalized our samples using the negative binomial distribution as recommended by McMurdie and Holmes(15) and implemented in the Bioconductor package DESeq2.[16] This approach simultaneously accounts for library size differences and biological variability. Between the RSV and sole RV groups, we compared the taxonomic α-diversity (OTU richness, Chao1, Shannon, ACE, Simpson, and Fischer indices) using linear regression models. We also examined the differences in microbial species abundances using the Wald test with Cook's distance correction for outliers (R *DESeq* package)(16) and adjusted by the Benjamini-Hochberg method to correct for multiple hypotheses testing at α=0.05.(17)

Microbiome functional profiling

We inferred the microbial gene functions and Gene Ontologies from the metatranscriptomic contigs annotated with Prokka (metagenomics mode).(18) Briefly, we removed the reads of human origin by mapping against the human genome sequence. Then, we assembled unmapped reads using the metaSpades algorithm and, after gene annotation, we mapped reads back to contigs (bowtie2) to estimate gene abundances. We estimated differential

gene expression using R *DESeq2*(16) and visualized using *ggplot2*.(19) Additionally, we also performed Gene Ontology enrichment analysis as implemented in topGO(20) to identify the most represented GO between the two groups.

Host gene expression

We compared the level of host gene expression using HISAT2 (hierarchical indexing for spliced alignment of transcripts) and Cufflinks.(21-23) First, we aligned the human mRNA reads to the human reference genome (hg19) in HISAT2.(21) We used gene annotations from the UCSC knownGene database(24) to facilitate the mapping process. We assembled the RNAseq alignments into potential transcripts using Cufflinks with the UCSC annotation guiding the transcriptome assembly. We also used this program to estimate the expressed gene abundance as fragments per kilobase of exon per million fragments mapped (fpkm) under default parameters. We computed bias-corrected gene and transcript expression profiles for each sample using Cuffquant and normalized the RNA-seq libraries using Cuffnorm. We calculated fold change, statistical significance, and examined differentially expressed host mRNAs between the RSV and sole RV groups by treating samples as biological replicates in Cuffdiff 2.(25)

Host pathway enrichment analysis

To understand the virus-specific effects on the host response in the airway, we carried out a host pathway enrichment analysis as implemented in GAGE.(26) We linked the human gene names to the KEGG pathways (R *gageData* package)(27) using only signaling and metabolic pathways. Then, we used the fold changes from the differential expression analysis as input of GAGE for the enrichment analysis.

Supplemental References

1. Hasegawa K, et al. Circulating 25-hydroxyvitamin D, nasopharyngeal airway metabolome, and bronchiolitis severity. Allergy 2018;73(5):1135–40.

2. Hasegawa K, et al. Nasopharyngeal CCL5 in infants with severe bronchiolitis and risk of recurrent wheezing: A multi-center prospective cohort study. Clin Exp Allergy 2018;48(8):1063–7.

3. Ralston SL, et al. Clinical practice guideline: The diagnosis, management, and prevention of bronchiolitis. Pediatrics 2014;134(5):e1474–502.

4. Marsh RL, et al. The microbiota in bronchoalveolar lavage from young children with chronic lung disease includes taxa present in both the oropharynx and nasopharynx. Microbiome 2016;4(1):37.

5. Charlson ES, et al. Topographical continuity of bacterial populations in the healthy human respiratory tract. Am J Respir Crit Care Med 2011;184(8):957–63.

6. Poole A, et al. Dissecting childhood asthma with nasal transcriptomics distinguishes subphenotypes of disease. J Allergy Clin Immunol 2014;133(3):670-678.e12.

7. Elden LJR van, et al. Applicability of a real-time quantitative PCR assay for diagnosis of respiratory syncytial virus infection in immunocompromised adults. J Clin Microbiol 2003;41(9):4378–81.

8. Kuypers J, et al. Comparison of real-time PCR assays with fluorescent-antibody assays for diagnosis of respiratory virus infections in children. J Clin Microbiol 2006;44(7):2382–8.

9. Lu X, et al. Real-time reverse transcription-PCR assay for comprehensive detection of human rhinoviruses. J Clin Microbiol 2008;46(2):533–9.

10. Schmieder R, Edwards R. Quality control and preprocessing of metagenomic datasets. Bioinformatics 2011;27(6):863–4.

11. Langmead B, Salzberg SL. Fast gapped-read alignment with Bowtie 2. Nat Methods 2012;9(4):357–9.

12. Francis OE, et al. Pathoscope: Species identification and strain attribution with unassembled sequencing data. Genome Res 2013;23(10):1721–9.

13. Byrd AL, et al. Clinical PathoScope: Rapid alignment and filtration for accurate pathogen identification in clinical samples using unassembled sequencing data. BMC Bioinformatics 2014;15(1):262.

14. Hong C, et al. PathoScope 2.0: A complete computational framework for strain identification in environmental or clinical sequencing samples. Microbiome 2014;2(1):33.

15. McMurdie PJ, Holmes S. Waste not, want not: Why rarefying microbiome data Is Inadmissible. PLoS Comput Biol 2014;10(4):e1003531.

16. Love MI, Huber W, Anders S. Moderated estimation of fold change and dispersion for RNA-seq data with DESeq2. Genome Biol 2014;15(12):550.

17. Benjamini Y, Hochberg Y. Controlling the false discovery rate - A practical and powerful approach to multiple testing. J R Stat Soc Ser B 1995;57:289–300.

18. Seemann T. Prokka: Rapid prokaryotic genome annotation. Bioinformatics 2014;30(14):2068–9.

19. H. Wickham. ggplot2: Elegant graphics for data analysis. Springer New York; 2009.

20. Alexa A, Rahnenfuhrer J. topGO: Enrichment analysis for gene ontology. R package version 2.36.0. 2019;

21. Kim D, Langmead B, Salzberg SL. HISAT: A fast spliced aligner with low memory requirements. Nat Methods 2015;12(4):357–60.

22. Trapnell C, et al. Differential gene and transcript expression analysis of RNA-seq experiments with TopHat and Cufflinks. Nat Protoc 2012;7(3):562–78.

23. Trapnell C, et al. Transcript assembly and quantification by RNA-Seq reveals unannotated transcripts and isoform switching during cell differentiation. Nat Biotechnol 2010;28(5):511–5.

24. UCSC Genome Browser Home [Internet]. [cited 2019 Sep 30];Available from: http://genome.ucsc.edu/

25. Trapnell C, et al. Differential analysis of gene regulation at transcript resolution with RNA-seq. Nat Biotechnol 2013;31(1):46–53.

26. Luo W, Friedman MS, Shedden K, Hankenson KD, Woolf PJ. GAGE: Generally applicable gene set enrichment for pathway analysis. BMC Bioinformatics 2009;10(1):161.

27. Luo W. gageData: Auxillary data for gage package. R package version 2.22.0. 2019;

Supplemental Table S1. Characteristics of infants hospitalized for bronchiolitis with respiratory syncytial virus infection or sole rhinovirus infection

Variables	RSV [a] (n=5)	Sole rhinovirus (n=5)	P-value
Characteristics			
Age (months), median (IQR)	4 (2-9)	10 (6-10)	0.25
Male sex	2 (40)	3 (60)	0.99
Race/ethnicity			0.99
Non-Hispanic white	2 (40)	2 (40)	
Non-Hispanic black	0 (0)	1 (20)	
Hispanic	2 (40)	2 (40)	
Other or unknown	1 (20)	0 (0)	
Maternal smoking during pregnancy	0 (0)	0 (0)	0.99
C-section delivery	1 (20)	3 (60)	0.52
Prematurity (32-37 weeks)	3 (60)	0 (0)	0.17
Previous breathing problems before the index hospitalization [b]	1 (20)	2 (40)	0.99
History of eczema	1 (20)	2 (40)	0.99
Ever attended daycare	3 (60)	1 (20)	0.52
Sibling in the household	3 (60)	3 (60)	0.99
Mostly breastfed for the first 3 mo of age	3 (60)	3 (60)	0.99
Smoke exposure at home	1 (20)	0 (0)	0.99
Corticosteroid use before the index hospitalization	0 (0)	1 (20)	0.99
Clinical presentation			
Weight at presentation (kg), median (IQR)	6.7 (5.6-8.2)	8.9 (7.9-9.4)	0.47
Respiratory rate at presentation (per minute), median (IQR)	60 (52-72)	48 (48-60)	0.40
Oxygen saturation at presentation			0.99
<90%	1 (20)	2 (40)	
90%-93%	1 (20)	0 (0)	
≥94%	3 (60)	3 (60)	
Received corticosteroids during prehospitalization visit	0 (0)	2 (40)	0.44

Abbreviations: RSV, respiratory syncytial virus; IQR, interquartile range.
Data are no. (%) of infants unless otherwise indicated.
Continuous variables were tested by Mann-Whitney U test. Categorical variables were tested by Fisher's exact test.
[a] Within the RSV group, RV was also detected in 2 patients.
[b] Defined as a child having cough that wakes him/her at night and/or causes emesis, or when the child has wheezing or shortness of breath without a cough.

ONLINE SUPPLEMENT December 2019

Supplemental Table S2. Microbiome Gene Ontology enrichment analysis in respiratory syncytial virus and sole rhinovirus infection groups

Respiratory syncytial virus			Sole rhinovirus		
GO ID	GO function	P-value	GO ID	GO function	P-value
Biological process					
0046083	adenine metabolic process	4.E-04	0040011	locomotion	2.E-03
0043096	purine nucleobase salvage	7.E-04	0002100	tRNA wobble adenosine to inosine editing	4.E-03
0006168	adenine salvage	8.E-04	0018065	protein-cofactor linkage	9.E-03
0046084	adenine biosynthetic process	8.E-04	0009405	pathogenesis	1.E-02
1902582	An intracellular transport which involves only one organism.	9.E-04	0001101	response to acid chemical	1.E-02
0043101	purine-containing compound salvage	1.E-03	0030420	establishment of competence for transformation	1.E-02
0006166	purine ribonucleoside salvage	1.E-03	0018160	peptidyl-pyrromethane cofactor link	1.E-02
0043174	nucleoside salvage	1.E-03	0015950	purine nucleotide interconversion	1.E-02
0009113	purine nucleobase biosynthetic process	2.E-03	0009432	SOS response	2.E-02
0006144	purine nucleobase metabolic process	2.E-03	0006164	purine nucleotide biosynthetic process	2.E-02
Cellular component					
0031522	cell envelope Sec protein transport complex	8.E-03	0045281	succinate dehydrogenase complex	1.E-02
0009279	cell outer membrane	8.E-03	0045282	plasma membrane succinate dehydrogenase complex	1.E-02
0019867	outer membrane	8.E-03	0044459	basolateral plasma membrane	2.E-02
0031469	polyhedral organelle	1.E-02	0045273	respiratory chain complex II	2.E-02
0031471	ethanolamine degradation polyhedral organelle	1.E-02	0045274	plasma membrane respiratory chain complex II	2.E-02
0009380	excinuclease repair complex	3.E-02	0070470	plasma membrane respiratory chain	2.E-02
0019197	phosphoenolpyruvate-dependent sugar phosphotransferase complex	4.E-02	0009321	alkyl hydroperoxide reductase activity	2.E-02
0043190	ATP-binding cassette (ABC) transporter complex	5.E-02	0044425	membrane part	4.E-02
0098533	ATPase dependent transmembrane transport complex	5.E-02	0098797	plasma membrane protein complex	4.E-02
0009358	polyphosphate kinase complex	6.E-03			
Molecular function					
0000010	trans-hexaprenyltranstransferase activity	3.E-04	0004000	adenosine deaminase activity	2.E-03

0008982	protein-N(PI)-phosphohistidine-sugar phosphotransferase activity	3.E-03	0008251	tRNA-specific adenosine deaminase activity	4.E-03
0005506	iron ion binding	4.E-03	0003985	acetyl-CoA C-acetyltransferase activity	5.E-03
0016763	transferase activity, transferring pentosyl groups	4.E-03	0004595	pantetheine-phosphate adenylyltransferase activity	6.E-03
0015144	carbohydrate transmembrane transporter activity	4.E-03	0071949	FAD binding	8.E-03
1901476	carbohydrate transporter activity	4.E-03	0016453	C-acetyltransferase activity	1.E-02
0015203	polyamine transmembrane transporter activity	9.E-03	0016408	C-acyltransferase activity	1.E-02
0015417	polyamine-transporting ATPase activity	9.E-03	0005102	signaling receptor binding	1.E-02
0004422	hypoxanthine phosphoribosyltransferase activity	1.E-02	0005186	pheromone activity	1.E-02
0016757	transferase activity, transferring glycosyl groups	1.E-02			

Abbreviation: GO, Gene Ontology

ONLINE SUPPLEMENT December 2019

Supplemental Table S3. Differentially-expressed host genes between respiratory syncytial virus infection compared to sole rhinovirus infection [a]

Genes	Log_2 fold change	P-value	q-value
TMEM88B	≥5	5.E-05	2.E-03
HES3	≥5	5.E-05	2.E-03
OPRD1	≥5	5.E-05	2.E-03
LOC339539	≥5	5.E-05	2.E-03
FOXD3	≥5	5.E-05	2.E-03
LCE2A	≥5	5.E-05	2.E-03
LCE1F	≥5	5.E-05	2.E-03
LCE1D	≥5	2.E-04	7.E-03
CCDC185	≥5	5.E-05	2.E-03
RNF186	≥5	5.E-05	2.E-03
LACTBL1	≥5	5.E-05	2.E-03
A3GALT2	≥5	5.E-05	2.E-03
ASCL5	≥5	5.E-05	2.E-03
PLAC9	≥5	5.E-05	2.E-03
NKX2-3	≥5	5.E-05	2.E-03
HMX3	≥5	5.E-05	2.E-03
HMX2	≥5	5.E-05	2.E-03
C10orf91	≥5	5.E-05	2.E-03
UTF1	≥5	5.E-05	2.E-03
GATA3-AS1	≥5	1.E-04	5.E-03
GDF10	≥5	5.E-05	2.E-03
NEUROG3	≥5	5.E-05	2.E-03
LBX1	≥5	5.E-05	2.E-03
PITX3	≥5	5.E-05	2.E-03
PRLHR	≥5	5.E-05	2.E-03
RBMXL2	≥5	5.E-05	2.E-03
MYOD1	≥5	5.E-05	2.E-03
MRGPRE	≥5	5.E-05	2.E-03
DBX1	≥5	5.E-05	2.E-03
GPR152	≥5	5.E-05	2.E-03
FGF4	≥5	5.E-05	2.E-03

FGF3	≥5	5.E-05	2.E-03
APOA4	≥5	5.E-05	2.E-03
H1FNT	≥5	5.E-05	2.E-03
HOXC12	≥5	5.E-05	2.E-03
C1QL4	≥5	5.E-05	2.E-03
LHX5	≥5	5.E-05	2.E-03
GSX1	≥5	5.E-05	2.E-03
ZIC2	≥5	5.E-05	2.E-03
DIO3	≥5	5.E-05	2.E-03
NKX2-8	≥5	5.E-05	2.E-03
CCDC177	≥5	5.E-05	2.E-03
ELK2AP	≥5	5.E-05	2.E-03
LOC100289656	≥5	5.E-05	2.E-03
FOXB1	≥5	5.E-05	2.E-03
LOC440311	≥5	5.E-05	2.E-03
OTUD7A	≥5	5.E-05	2.E-03
ANKRD63	≥5	5.E-05	2.E-03
RNF151	≥5	5.E-05	2.E-03
TRIM72	≥5	3.E-04	1.E-02
LINC00235	≥5	5.E-05	2.E-03
C1QTNF8	≥5	5.E-05	2.E-03
PLA2G10	≥5	5.E-05	2.E-03
ZNF843	≥5	5.E-05	2.E-03
BHLHA9	≥5	5.E-05	2.E-03
RNF126P1	≥5	5.E-05	2.E-03
GALR2	≥5	5.E-05	2.E-03
UTS2R	≥5	5.E-05	2.E-03
ASIC2	≥5	2.E-04	9.E-03
NEUROD2	≥5	5.E-05	2.E-03
KRTAP2-1	≥5	5.E-05	2.E-03
HCRT	≥5	5.E-05	2.E-03
SOST	≥5	5.E-05	2.E-03
C1QL1	≥5	5.E-05	2.E-03

RPRML	≥5	5.E-05	2.E-03
BTBD17	≥5	5.E-05	2.E-03
MYADML2	≥5	5.E-05	2.E-03
NOTUM	≥5	5.E-05	2.E-03
CIDEA	≥5	2.E-04	7.E-03
SALL3	≥5	5.E-05	2.E-03
RAX	≥5	5.E-05	2.E-03
LOC644189	≥5	5.E-05	2.E-03
SELV	≥5	5.E-05	2.E-03
IRGC	≥5	5.E-05	2.E-03
C19orf81	≥5	2.E-04	7.E-03
ZNF534	≥5	2.E-04	9.E-03
ODF3L2	≥5	5.E-05	2.E-03
RAX2	≥5	5.E-05	2.E-03
ACTL9	≥5	5.E-05	2.E-03
LGI4	≥5	5.E-05	2.E-03
SHANK1	≥5	5.E-05	2.E-03
SBK2	≥5	5.E-05	2.E-03
SBK3	≥5	5.E-05	2.E-03
VAX2	≥5	5.E-05	2.E-03
EMX1	≥5	5.E-05	2.E-03
NOTO	≥5	5.E-05	2.E-03
POU3F3	≥5	5.E-05	2.E-03
FOXD4L1	≥5	5.E-05	2.E-03
HOXD12	≥5	5.E-05	2.E-03
HOXD4	≥5	5.E-05	2.E-03
NEU2	≥5	5.E-05	2.E-03
NTSR2	≥5	5.E-05	2.E-03
EN1	≥5	5.E-05	2.E-03
FEV	≥5	5.E-05	2.E-03
GBX2	≥5	5.E-05	2.E-03
AQP12B	≥5	5.E-05	2.E-03
SSTR4	≥5	5.E-05	2.E-03

SCRT2	≥5	5.E-05	2.E-03
ADRA1D	≥5	5.E-05	2.E-03
LRRN4	≥5	5.E-05	2.E-03
NKX2-4	≥5	5.E-05	2.E-03
VSX1	≥5	4.E-04	2.E-02
BHLHE23	≥5	5.E-05	2.E-03
GAL3ST1	≥5	5.E-05	2.E-03
MOBP	≥5	4.E-04	1.E-02
SOX14	≥5	5.E-05	2.E-03
FOXL2	≥5	5.E-05	2.E-03
PRR23B	≥5	5.E-05	2.E-03
GPR78	≥5	2.E-04	7.E-03
DRD5	≥5	5.E-05	2.E-03
ZAR1	≥5	5.E-05	2.E-03
GSX2	≥5	5.E-05	2.E-03
ATOH1	≥5	5.E-05	2.E-03
HELT	≥5	5.E-05	2.E-03
NKX1-1	≥5	5.E-05	2.E-03
HMX1	≥5	5.E-05	2.E-03
NKX3-2	≥5	5.E-05	2.E-03
LINC01096	≥5	5.E-05	2.E-03
NKX6-1	≥5	5.E-05	2.E-03
PITX2	≥5	1.E-03	5.E-02
NEUROG2	≥5	5.E-05	2.E-03
WWC2-AS2	≥5	5.E-05	2.E-03
LRRC14B	≥5	5.E-05	2.E-03
POU4F3	≥5	5.E-05	2.E-03
ADRA1B	≥5	5.E-05	2.E-03
TLX3	≥5	5.E-05	2.E-03
OTP	≥5	5.E-05	2.E-03
LOC389332	≥5	5.E-05	2.E-03
HDGFL1	≥5	5.E-05	2.E-03
OLIG3	≥5	5.E-05	2.E-03

VWC2	≥5	5.E-05	2.E-03
POM121L12	≥5	5.E-05	2.E-03
HOXA3	≥5	3.E-04	1.E-02
GBX1	≥5	5.E-05	2.E-03
SHH	≥5	5.E-05	2.E-03
FGF17	≥5	5.E-05	2.E-03
NPBWR1	≥5	5.E-05	2.E-03
REXO1L2P	≥5	5.E-05	2.E-03
FAM90A25P	≥5	5.E-05	2.E-03
NKX2-6	≥5	1.E-04	5.E-03
ADRB3	≥5	5.E-05	2.E-03
GPR20	≥5	5.E-05	2.E-03
CCDC166	≥5	5.E-05	2.E-03
SCRT1	≥5	5.E-05	2.E-03
KCNV2	≥5	5.E-05	2.E-03
FOXB2	≥5	5.E-05	2.E-03
BARHL1	≥5	5.E-05	2.E-03
ACTL7B	≥5	5.E-05	2.E-03
FAM163B	≥5	5.E-05	2.E-03
NYX	≥5	5.E-05	2.E-03
FRMD8P1	≥5	5.E-05	2.E-03
SOX3	≥5	5.E-05	2.E-03
PCDHA	≥5	5.E-05	2.E-03
KIF26A	4.7	5.E-04	2.E-02
TRIL	4.4	1.E-03	4.E-02
SOWAHA	4.2	1.E-03	4.E-02
C9orf172	4.1	2.E-03	5.E-02
FABP3	4.0	4.E-04	2.E-02
NAT8L	3.9	3.E-04	1.E-02
BAI1	3.7	2.E-03	5.E-02
KIF26B	3.6	1.E-03	4.E-02
CSPG4	3.6	9.E-04	3.E-02
TRIM36	3.5	9.E-04	3.E-02

LPL	3.5	5.E-05	2.E-03
MN1	3.4	5.E-05	2.E-03
MFGE8	3.4	6.E-04	2.E-02
NTSR1	3.2	1.E-03	4.E-02
VGF	3.1	8.E-04	3.E-02
PCDHG	3.1	5.E-05	2.E-03
PROB1	3.1	5.E-05	2.E-03
MUC15	3.0	1.E-03	4.E-02
ZNF469	3.0	5.E-05	2.E-03
ZFP41	2.9	2.E-04	9.E-03
INSM1	2.9	2.E-03	5.E-02
WWOX	2.8	8.E-04	3.E-02
LINC00265	2.8	5.E-05	2.E-03
METTL21A	2.7	5.E-05	2.E-03
PPIL6	2.6	2.E-04	7.E-03
MMP9	2.6	5.E-05	2.E-03
ZNF74	2.5	5.E-05	2.E-03
DAGLA	2.5	5.E-04	2.E-02
LINC00957	2.5	1.E-03	4.E-02
PADI1	2.5	9.E-04	3.E-02
BAHCC1	2.5	5.E-05	2.E-03
NEURL1	2.4	1.E-03	4.E-02
PLCH2	2.4	6.E-04	2.E-02
LOC729218	2.4	1.E-03	4.E-02
FJX1	2.4	2.E-03	5.E-02
ZNF628	2.4	7.E-04	3.E-02
C19orf68	2.4	1.E-03	3.E-02
B3GNT6	2.3	9.E-04	3.E-02
P2RY1	2.3	1.E-03	4.E-02
NHLRC4	2.3	7.E-04	2.E-02
MMP8	2.3	1.E-03	3.E-02
MAP9	2.3	5.E-05	2.E-03
DSG2	2.3	4.E-04	2.E-02

HSD11B1L	2.3	2.E-04	7.E-03
HP	2.2	5.E-04	2.E-02
SNAPC4	2.2	1.E-03	4.E-02
GLTSCR1	2.2	5.E-05	2.E-03
SHANK3	2.2	6.E-04	2.E-02
IRX3	2.2	1.E-03	4.E-02
AHDC1	2.1	1.E-04	5.E-03
SP6	2.1	1.E-03	3.E-02
CXADR	2.1	5.E-05	2.E-03
NUPR1	2.1	5.E-04	2.E-02
KCNC4	2.0	7.E-04	2.E-02
PSMG3-AS1	2.0	5.E-04	2.E-02
MAP3K19	2.0	3.E-04	1.E-02
PKD1P1	2.0	2.E-04	7.E-03
GAS2L1	2.0	6.E-04	2.E-02
CTGF	1.9	2.E-04	7.E-03
DNAL1	1.9	6.E-04	2.E-02
VTCN1	1.9	6.E-04	2.E-02
AHNAK2	1.9	3.E-04	1.E-02
VNN1	1.9	3.E-04	1.E-02
CRISPLD2	1.9	7.E-04	3.E-02
ARMC5	1.9	2.E-03	5.E-02
HIC2	1.8	1.E-03	3.E-02
CYP51A1	1.8	7.E-04	2.E-02
EPPK1	1.8	5.E-05	2.E-03
KIAA1161	1.8	6.E-04	2.E-02
RSPH4A	1.8	1.E-03	4.E-02
RPS16	1.6	4.E-04	1.E-02
FAM216B	1.4	1.E-03	4.E-02
NDST1	1.4	1.E-03	5.E-02
RHOU	1.3	1.E-03	5.E-02
HIST1H2AM	-1.4	2.E-03	5.E-02
HIST1H3G	-1.4	2.E-03	5.E-02

HIST1H2AE	-1.4	1.E-03	4.E-02
HIST1H4H	-1.4	1.E-03	4.E-02
PPP1R16B	-1.4	2.E-03	5.E-02
HIST1H3J	-1.4	1.E-03	5.E-02
HIST2H3D	-1.4	1.E-03	5.E-02
HLA-DRB1	-1.4	1.E-03	4.E-02
HIST1H2BI	-1.5	1.E-03	4.E-02
HIST1H3C	-1.5	9.E-04	3.E-02
HIST1H2AB	-1.5	1.E-03	4.E-02
HIST1H3F	-1.5	6.E-04	2.E-02
HIST1H2AH	-1.5	9.E-04	3.E-02
HIST1H2AG	-1.6	4.E-04	1.E-02
ANXA6	-1.6	2.E-03	5.E-02
PTPRCAP	-1.7	7.E-04	3.E-02
C20orf27	-1.7	1.E-03	5.E-02
RFTN1	-1.7	9.E-04	3.E-02
HIST1H2BB	-1.7	1.E-03	4.E-02
HIST1H1B	-1.7	5.E-05	2.E-03
HIST1H3B	-1.8	1.E-04	5.E-03
AKR1B1	-1.8	2.E-04	9.E-03
BPI	-1.8	9.E-04	3.E-02
IRF8	-1.8	5.E-05	2.E-03
CDC42EP2	-1.8	2.E-04	7.E-03
HIST1H2AI	-1.8	5.E-05	2.E-03
MAP3K14	-1.9	3.E-04	1.E-02
SPIB	-2.2	1.E-04	5.E-03
SPN	-2.3	1.E-04	5.E-03
CD79B	-2.3	1.E-03	4.E-02
FCRLA	-2.5	5.E-05	2.E-03
POU2AF1	-2.5	5.E-05	2.E-03
ELANE	-2.6	2.E-04	7.E-03
PRTN3	-2.7	6.E-04	2.E-02
DEFA1	-2.8	5.E-05	2.E-03

FAM107A	-2.8	4.E-04	2.E-02
IGJ	-2.8	5.E-04	2.E-02
MPO	-2.9	5.E-05	2.E-03
AZU1	-2.9	5.E-05	2.E-03
CXCL13	-2.9	2.E-04	9.E-03
CR2	-3.2	5.E-05	2.E-03
SPARC	-4.0	5.E-05	2.E-03

[a] Expression of 269 genes were significantly (q-value <0.05) different.

Supplemental Table S4. Significantly-enriched pathways in respiratory syncytial virus and sole rhinovirus infection group

Pathway name	p-value	q-value
RSV group a		
Hedgehog signaling (hsa04340)	3.E-05	5.E-03
Calcium signaling (hsa04020)	5.E-04	4.E-02
Solo RV group b		
Ribosome (hsa03010)	3.E-16	5.E-14
Spliceosome (hsa03040)	2.E-09	2.E-07
RNA transport (hsa03013)	3.E-09	2.E-07
Cell cycle (hsa04110)	3.E-08	1.E-06
Osteoclast differentiation (hsa04380)	3.E-08	1.E-06
Oxidative phosphorylation (hsa00190)	3.E-07	8.E-06
Ubiquitin mediated proteolysis (hsa04120)	7.E-07	2.E-05
B cell receptor signaling pathway (hsa04662)	6.E-06	1.E-04
DNA replication (hsa03030)	1.E-05	1.E-04
Chemokine signaling pathway（hsa04062)	1.E-05	1.E-04
Pyrimidine metabolism (hsa00240)	1.E-05	1.E-04
Ribosome biogenesis in eukaryotes (hsa03008)	2.E-05	2.E-04
Phagosome (hsa04145)	4.E-05	4.E-04
Antigen processing and presentation (hsa04612)	4.E-05	4.E-04
Fc gamma R-mediated phagocytosis (hsa04666)	5.E-05	5.E-04
Toll-like receptor signaling pathway (hsa04620)	7.E-05	7.E-04
RNA degradation (hsa03018)	9.E-05	9.E-04
p53 signaling pathway (hsa04115)	2.E-04	2.E-03
Proteasome (hsa03050)	2.E-04	2.E-03
T cell receptor signaling pathway (hsa04660)	2.E-04	2.E-03
Jak-STAT signaling pathway (hsa04630)	2.E-04	2.E-03
NOD-like receptor signaling pathway (hsa04621)	3.E-04	2.E-03
Nucleotide excision repair (hsa03420)	4.E-04	3.E-03
Natural killer cell mediated cytotoxicity (hsa04650)	4.E-04	3.E-03
Apoptosis (hsa04210)	5.E-04	3.E-03
mRNA surveillance pathway (hsa03015)	6.E-04	4.E-03
Cytosolic DNA-sensing pathway (hsa04623)	6.E-04	4.E-03
Protein processing in endoplasmic reticulum (hsa04141)	7.E-04	4.E-03
Lysosome (hsa04142)	9.E-04	5.E-03
Oocyte meiosis (hsa04114)	1.E-03	6.E-03
Base excision repair (hsa03410)	1.E-03	7.E-03
Neurotrophin signaling pathway (hsa04722)	1.E-03	7.E-03
Focal adhesion (hsa04510)	1.E-03	7.E-03
Mismatch repair (hsa03430)	2.E-03	1.E-02

Insulin signaling pathway (hsa04910)	2.E-03	1.E-02
Homologous recombination (hsa03440)	2.E-03	1.E-02
Metabolism of xenobiotics by cytochrome P450 (hsa00980)	3.E-03	2.E-02
RIG-I-like receptor signaling pathway (hsa04622)	4.E-03	2.E-02
Drug metabolism - cytochrome P450 (hsa00982)	5.E-03	2.E-02
Glycolysis / Gluconeogenesis (hsa00010)	5.E-03	2.E-02
Glutathione metabolism (hsa00480)	5.E-03	2.E-02
Citrate cycle (TCA cycle) (hsa00020)	6.E-03	2.E-02
RNA polymerase (hsa03020)	9.E-03	3.E-02
Fructose and mannose metabolism (hsa00051)	9.E-03	3.E-02
Progesterone-mediated oocyte maturation (hsa04914)	1.E-02	4.E-02
Fc epsilon RI signaling pathway (hsa04664)	1.E-02	4.E-02
mTOR signaling pathway (hsa04150)	1.E-02	4.E-02
Purine metabolism (hsa00230)	1.E-02	5.E-02
Aminoacyl-tRNA biosynthesis (hsa00970)	1.E-02	5.E-02

[a] 2 pathways were significantly (q-value <0.05) enriched.
[b] 49 pathways were significantly (q-value <0.05) enriched.

ONLINE SUPPLEMENT December 2019

Supplemental Figure S1. Comparisons of α-diversity measures between respiratory syncytial virus and sole rhinovirus infection groups

Although Shannon and Simpson indices appeared higher in the RSV group, there were no statistically significant differences (all P>0.05).

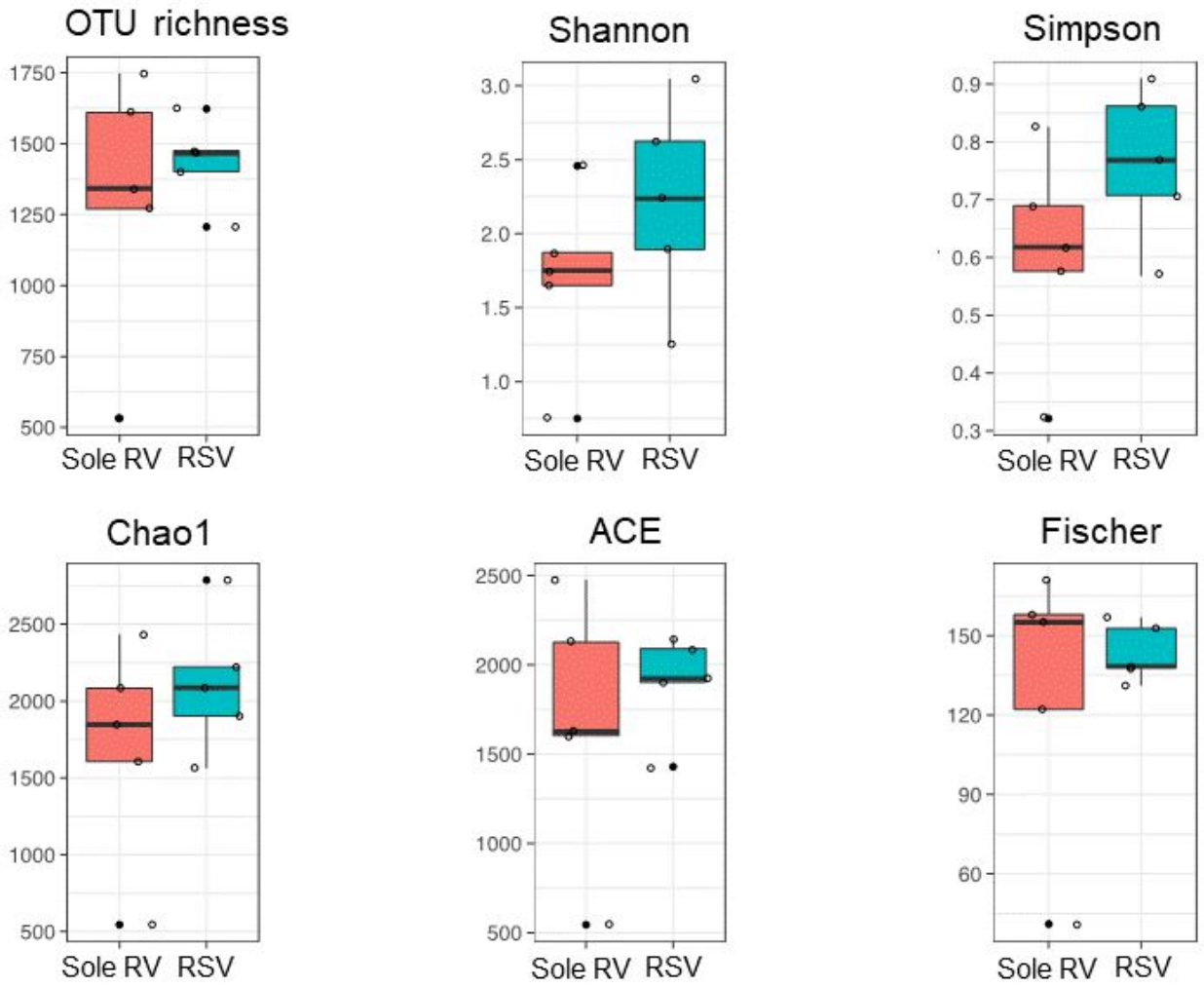

Abbreviations: RSV, respiratory syncytial virus; RV, rhinovirus.

ONLINE SUPPLEMENT December 2019

Supplemental Figure S2. Differential microbial species abundance in the nasopharyngeal airway microbiome between respiratory syncytial virus and sole rhinovirus groups

Differentially-abundant species in the RSV group are represented by positive fold changes, while those in the sole RV group are represented by negative fold changes.